Atmos. Chem. Phys. Discuss., 3, 3222–3240, 2003
www.atmos-chem-phys.org/acpd/3/3222/

Atmospheric Chemistry and Physics Discussions

The North Atlantic Oscillation controls air pollution transport to the Arctic

S. Eckhardt[1], A. Stohl[1], S. Beirle[2], N. Spichtinger[1], P. James[1], C. Forster[1], C. Junker[3], T. Wagner[2], U. Platt[2], and S. G. Jennings[3]

[1]Department of Ecology, Technical University of Munich, Germany
[2]Institute of Environmental Physics, Heidelberg University, Germany
[3]Department of Experimental Physics, National University of Ireland, Ireland

Received: 4 April 2003 – Accepted: 12 June 2003 – Published: 24 June 2003

Correspondence to: A. Stohl (stohl@forst.tu-muenchen.de)

Abstract

This paper studies the interannual variability of pollution pathways from northern hemisphere (NH) continents into the Arctic. Using a 15-year model simulation of the dispersion of passive tracers representative of anthropogenic emissions from NH continents, we show that the North Atlantic Oscillation (NAO) exerts a strong control on the pollution transport into the Arctic, particularly in winter and spring. For tracer lifetimes of 5 (30) days, surface concentrations in the Arctic winter are enhanced by about 70% (30%) during high phases of the NAO (in the following referred to as NAO^+) compared to its low phases (NAO^-). This is mainly due to great differences in the pathways of European pollution during NAO^+ and NAO^- phases, respectively, but reinforced by North American pollution, which is also enhanced in the Arctic during NAO^+ phases. In contrast, Asian pollution in the Arctic does not significantly depend on the NAO phase. The model results are confirmed using remotely-sensed NO_2 vertical atmospheric columns obtained from seven years of satellite measurements, which show enhanced northward NO_2 transport and reduced NO_2 outflow into the North Atlantic from Central Europe during NAO^+ phases. Surface measurements of carbon monoxide (CO) and black carbon at high-latitude stations further corroborate the overall picture of enhanced Arctic pollution levels during NAO^+ phases.

1. Introduction

During winter and spring, the Arctic suffers from high levels of anthropogenic pollution (Mitchell, 1957), leading to decreased visibility – the Arctic haze (Barrie, 1986) – radiative forcing of the Arctic climate (Garrett et al., 2002), soil pollution (Meijer et al., 2003), and accumulation of persistent organic chemicals (Wania, 2003). Accumulation of ozone precursors in the Arctic in winter and their release to lower latitudes in spring also causes a peak in photochemical ozone formation, contributing to the spring-time maximum in photooxidants that is observed throughout much of the north-

ACPD
3, 3222–3240, 2003

ern hemisphere (NH) troposphere (Penkett and Brice, 1986). Factors that cause the winter/spring maximum of Arctic pollution, i.e. seasonal changes in pollutant removal rates, photochemical processes, local meteorology and pollution transport pathways, are reasonably well understood now (Barrie, 1986; Polissar et al., 2001). There is also evidence for downward trends of, e.g. sulfate, cadmium, or aerosol scattering, that have been related to emission reductions (Bodhaine, 1989; Li et al., 2003). However, little attention has yet been paid to the influence of climate variability on interannual changes of Arctic air pollution levels.

In the NH, especially during the winter months, the most prominent and recurrent pattern of atmospheric variability is the North Atlantic Oscillation (NAO), a redistribution of atmospheric mass between the Arctic and the subtropical Atlantic (Hurrell, 1995). Oscillations between high and low NAO phases produce large changes in the mean wind speed and direction over the Atlantic, the heat and moisture transport between the Atlantic and the neighbouring continents, and the intensity and number of storms (Hurrell et al., 1997). Thus, NAO-related influences on hemispheric-scale pollution transport are to be expected. Indeed, it has been shown that the NAO influences the transport of Saharan dust into the Atlantic and Mediterranean (Moulin et al., 1997), and photochemical model calculations suggest that it may also modify the transport of pollutants from North America to Europe (Li et al., 2002). Here we present a significant correlation between the NAO and air pollution transport towards the Arctic. The results of this paper represent the strongest signal found in a survey of the dependence of global pollution transport pathways on a series of popular indices describing climate variability in various regions of the globe (the Southern Oscillation, Pacific-North America pattern, Arctic Oscillation and NAO).

2. Methods

Poleward transport of air pollution was examined in a 15-year (1979–1993) climatology, an extension to a previous one-year study (Stohl et al., 2002). The climatology is based

on calculations with the Lagrangian particle dispersion model FLEXPART (Stohl et al., 1998), driven by six-hourly meteorological re-analysis data from the European Centre for Medium-Range Weather Forecasts (ECMWF) (Gibson et al., 1999). The transport of three (Asian, European, North American) carbon monoxide (CO) pollution tracers was simulated. Emissions were taken from the global EDGAR version 2 inventory (Olivier et al., 1996) with the base year 1990. Attribution of an EDGAR grid cell to a particular continent was done approximately according to the continental boundaries shown on a geographical map, resulting in the emission distribution shown in Fig. 1. Anthropogenic CO emissions have a distribution similar to the emissions of many other anthropogenic pollutants, and thus are used here also as a proxy for anthropogenic pollution in a general sense.

Tracer particles were tagged with their release time and followed in the simulation for 50 days. Resulting tracer concentrations were binned into 12 age classes and stored on a three-dimensional grid as monthly averages. Thus, for every month of our simulation, 12 concentration fields, each one consisting of tracer of definite age only (e.g. 0–2 days for the "youngest" age class, and 40–50 days for the "oldest" age class) were available for further analyses. This age-spectrum approach, which is popular in stratospheric research (Hall and Plumb, 1994), is useful for a posteriori determining approximately the concentrations of tracers with different e-folding lifetimes. Chemical species in the atmosphere can be characterized by their lifetime τ, after which their mass has decreased to 1/e of its initial value (i.e. the mass emitted). To determine the concentration C of a species with lifetime τ from the discrete age spectra, we can use

$$C \approx \sum_{n=1}^{N} C_n e^{-\frac{t_n}{\tau}} \quad , \tag{1}$$

where C_n is the tracer concentration in the age class n, t_n is the mean age of class n, and N is the number of age classes used (12 in our case). This approximate relationship holds for species with lifetimes well within the range of the age classes available.

The age spectra can also be used conveniently to create movies (each consisting

of N frames) of time-mean tracer dispersion. This can be done either for an individual month (note that we have monthly model output), or for suitably defined ensembles of individual months (furtheron referred to as composites). To obtain the composites, the age spectra of the months pertaining to the ensemble are simply averaged. In order to study the NAO's influence on tracer transport, we have produced composite movies representing ensemble averages of the winter months with the highest (hereafter referred to as NAO^+) and lowest (NAO^-) 20% of all NAO indices (mean values of these ensembles are 3.6 and −3.0, respectively). The NAO index used here was derived from the difference of normalized sea level pressure (SLP) between Ponta Delgada, Azores and Stykkisholmur/Reykjavik, Iceland (Hurrell, 1995). The monthly NAO index values were taken from an internet website (http://www.cgd.ucar.edu/~jhurrell/nao.html).

3. Results

Figure 2 shows snapshots from the two dispersion movies of the European tracer for composites based on months with NAO^+ conditions and months with NAO^- conditions, respectively. The full movies showing the dispersion of the European, Asian and North American tracers are available from http://www.forst.tu-muenchen.de/EXT/LST/METEO/arcticpollution. After 2-4 days (Figs. 2a, b), the European pollution plume is largely confined to south of 60° N for NAO^-, but it reaches 70° N for NAO^+. After 8–10 days (Figsb. 2c, d), most of the European tracer is found south (north) of the Arctic circle for the NAO^- (NAO^+) composites. In the movies, large differences between the two NAO phases are evident for up to 25 days, after which the differences decrease. Thus, while European pollution is eventually transported to the Arctic under both regimes, the poleward transport is faster during NAO^+ phases.

Figure 3 shows the corresponding plots for the North America tracer. Like for the European tracer, more North American tracer reaches Arctic latitudes during NAO^+ phases, even though the differences between the two composites are smaller. The tracer's transport across the North Atlantic is faster and directed towards higher lat-

ACPD
3, 3222–3240, 2003

itudes during for the NAO^+ ensemble. Transport of North American air pollution is strongly affected by the warm conveyor belt airstreams of extratropical cyclones (Stohl et al., 2002), and these warm conveyor belts show a similar correlation with the NAO (Eckhardt et al., 2003).

In order to quantify the contributions of European, Asian and North American emissions to the Arctic pollution, we plot for both NAO phases the average tracer mixing ratios at the surface, averaged over the Arctic region north of 70° N, in dependence of the tracer's e-folding lifetime. Figure 4 reveals three important facts: Firstly, European emissions contribute more to Arctic pollution than Asian and North American emissions together, due to Europe's position at higher latitudes and prevailing airflow patterns (Stohl et al., 2002). Secondly, more tracer from all three source continents is found in the Arctic for NAO^+ than for NAO^-. Thirdly, the NAO dependence is strongest for the European tracer and decreases with its e-folding lifetime. For an e-folding lifetime of 5 days (30 days), 90% (50%) more European tracer and 70% (30%) more tracer in total resides in the Arctic for NAO^+ than for NAO^-.

Fig. 5 shows maps of the slopes between the surface mixing ratios of the 30-day-lifetime tracers (from all NH continents together, as well as from Europe, America, and Asia alone), and the NAO index, obtained from a linear regression analysis. Both the North American tracer and the European tracer show a bipole pattern, with a region of positive slopes north of the main source region, and a region with negative slopes south of the source region (note the difference in scale, though, between panels b and c). The slopes for the Asian tracer reveal a more complicated distribution, which is largely not significant, but in the polar regions positive slopes are found, too. The slopes for tracer mixing ratios originating from all NH continents together closely resemble the results for Europe alone, confirming the dominant European signal.

To prove that the NAO affects the pollution outflow from Europe as suggested by the model, we use satellite measurements of a short-lived (lifetime of hours in the boundary layer, and up to a few days in the free troposphere) substance, nitrogen dioxide (NO_2), from the Global Ozone Monitoring Experiment (GOME). GOME is a spectrom-

eter operating in nadir-viewing geometry on the ERS-2 satellite since 1995 (Burrows et al., 1999). From the spectral data, total column NO_2 is retrieved using Differential Optical Absorption Spectroscopy (Leue et al., 2001). Residual NO_2 columns for NAO^+ minus NAO^- conditions, constructed from monthly data for seven winters (ensemble-mean NAO indices were −2.1 and 2.0, respectively), show a dipole structure with a NO_2 surplus over northern Europe and a deficit over western Europe (Fig. 6a). Careful analyses of cloud data from GOME itself, the International Satellite Cloud Climatology Project (Rossow and Schiffer, 1999), and ECMWF tropopause heights for NAO^+ and NAO^- conditions revealed no correspondence to the identified spatial structures. Thus, the NO_2 residuals are no artifact of the retrieval technique, but really show an enhanced outflow into the Arctic and a decreased outflow into the North Atlantic of European pollution for the NAO^+ compared to the NAO^- ensemble. A map of NAO^+ minus NAO^- residuals of the European 1-day-lifetime tracer columns (Fig. 6b) corroborates this finding. Even though the time periods of the model simulations and the measurements do not overlap and the model does not account for chemical transformations and deposition (other than applying a 1-day lifetime), there is very good agreement between the two maps. The spatial patterns identified in the model results are statistically highly significant, with correlation coefficients between the NAO indices and the tracer columns of between −0.79 and 0.68.

Unfortunately, NO_2 has too short a lifetime to trace the pollution all the way into the Arctic. However, in-situ measurements of longer-lived substances at high-latitude stations confirm our model results. Table 1 shows results of a linear correlation analysis of CO data at three Arctic stations (Spitsbergen, Barrow, Alert) and at the Irish west coast (Mace Head), obtained from the NOAA global flask sampling network (Novelli et al., 1998), and black carbon (BC) data (Cooke et al., 1997) at Mace Head. CO (BC) has a lifetime of several months (about 10 days) in Arctic winter. Since all timeseries show a downward trend, which is not discussed further here, a multiple linear regression was performed with both time and the NAO index as independent variables, in order to exclude the possibility that correlations are due to joint NAO and emission

trends. However, at all stations the NAO index is the main explanatory variable, and thus a regression with the NAO index alone yields very similar correlations and slopes. Depending on the station, the analysis explains about 30-50% of the variability seen in the data. At the Irish Mace Head research station, close to the negative pole in Fig. 6, there is a modest negative correlation between NAO and CO. According to the model simulations, this is a superposition of a strong negative correlation with European CO and a weaker positive correlation with North American CO (Fig. 5). For the shorter-lived BC, for which the North American influence is small, we see a very strong and highly significant negative correlation with the NAO, reflecting reduced outflow from Europe to the North Atlantic during NAO^+ phases.

In contrast, highly significant positive correlations between NAO and CO are found at all Arctic stations, confirming the enhanced poleward transport of air pollution from Europe and North America during NAO^+ phases, seen in Figs. 1–4. For NAO indices of −4 (+4), CO is nearly 10% lower (higher) than on average. Fig. 5 demonstrates that most of this correlation can be explained by NAO-related modifications of European pollution transport.

Similar, albeit weaker, correlations between the NAO and both measurement data and model results were found for spring, whereas for summer and autumn low correlations were obtained. This is expected, as the NAO is strongest in winter and early spring (Hurrell et al., 1997). Similar correlations were found with alternative NAO-related patterns like the Arctic Oscillation. The NAO was used here because European emissions are most important for Arctic air pollution and the NAO possesses the greatest explanatory power over the Euro-Atlantic region (Ambaum et al., 2001).

4. Discussion and conclusions

Using a 15-year tracer transport climatology it was found in this study that transport of anthropogenic pollution from all three NH continents correlates with the NAO in winter (and spring). Enhanced transport of pollution to the Arctic from all three NH continents

was observed during high NAO phases. The strongest dependency of simulated Arctic pollution levels on the NAO occurred for the pollution originating from Europe, and the correlation with the NAO index was strongest for tracers with short lifetimes. Satellite observations of NO_2 show a similar correlation with the NAO index and, thus, confirm the model results. CO measurements at Arctic surface stations, which are all positively correlated with the NAO, further corroborate our model results.

Our observation that the NAO controls pollution outflow from NH continents into the Arctic has important consequences. During the past decades, there has been a positive trend in the NAO (Hurrell, 1995), explaining partly why climate change in the Arctic was probably faster than anywhere else in the world (Moritz et al., 2002). Anthropogenic aerosols reduce cloud droplet sizes (Bréon et al., 2002), which globally leads to negative radiative forcing due to an increase in cloud reflectivity. However, under Arctic conditions (large solar zenith angles, high surface albedo because of snow and ice), aerosols warm the surface by increasing the longwave emissivity of thin clouds (Garrett et al., 2002), which adds to the forcing by greenhouse gases. Thus, part of the observed Arctic warming may have been due to enhanced transport of anthropogenic pollution into the Arctic during the past decades, both because of increasing emissions and the positive NAO trend. Very recently, though, the Arctic has cooled and become less cloudy in winter (Wang and Key, 2003), which could be related to recent emission reductions in Europe and North America, and a stabilization of the NAO in the last decade.

Another implication of our results is a possible feedback on the NAO itself, caused by transport of short-lived greenhouse gases and aerosols to the Arctic varying with the NAO phase. Both the strength and the direction of such a feedback loop are unknown yet, but could possibly be explored with chemistry-climate models.

According to our results, the NAO may lead to large interannual and decadal variability of nitrogen deposition to the Arctic Ocean, with potentially important ecological implications (Pearl et al., 1999). Furthermore, a negative correlation between the NAO and nitrate concentrations in UK freshwaters has been reported, but is not yet explained

ACPD
3, 3222–3240, 2003

(Monteith et al., 2000). We suggest that variability in atmospheric pollution transport may be responsible.

Acknowledgements. This study was funded by the German Federal Ministry for Education and Research within the Atmospheric Research Program 2000 (AFO 2000) as part of the projects CARLOTTA and NOXTRAM. ECMWF and the German Weather Service permitted access to the ECMWF archives. We acknowledge the National Oceanic and Atmospheric Administration (NOAA), Climate Monitoring and Diagnostics Laboratory (CMDL), Carbon Cycle Group, for providing CO data on the web, and J. Hurrell from the Climate Analysis Section, NCAR, Boulder, USA, for the NAO index data. Support of the BC measurement programme by T. Gerard Spain at Mace Head is gratefully acknowledged. We also wish to acknowledge support from the EU through the 5FP Project: CORE (Climate-Biosphere-Interactions), Contract number: EVRI-CT1999-40009.

References

Ambaum, M. H. P., Hoskins, B. J., and Stephenson, D. B.: Arctic Oscillation or North Atlantic Oscillation?, J. Climate, 14, 3495–3507, 2001. 3229

Barrie, L. A.: Arctic air-pollution – an overview of current knowledge, Atmos. Environ., 20, 643–663, 1986. 3223, 3224

Bodhaine, B. A.: Barrow surface aerosol: 1976–1987, Atmos. Environ., 23, 2357–2369, 1989. 3224

Bréon, F.-M., Tanré, D., and Generoso, S.: Aerosol effect on cloud droplet size monitored from satellite, Science, 295, 834–838, 2002. 3230

Burrows, J. P., Weber, M. Buchwitz, M., Rozanov, V. V., Ladstätter, A., Weißenmayer, Richter, A., DeBeek, R., Hoogen, R., Bramstedt, K., and Eichmann, K. U.: The Global Ozone Monitoring Experiment (GOME): Mission concept and first scientific results, J. Atmos. Sci., 56, 151–175, 1999. 3228

Cooke, W. F., Jennings, S. G., and Spain, T. G.: Black carbon measurements at Mace Head, 1989–1996, J. Geophys. Res., 102, 25 339–25 346, 1997. 3228

Eckhardt, S., Stohl, A., Wernli, H., James, P., Forster, C., and Spichtiner, N.: A 15-year climatology of warm conveyor belts, J. Climate, submitted, 2003. 3227

Garrett, T. J., Radke, L. F., and Hobbs, P. V.: Aerosol effects on cloud emissivity and surface longwave heating in the Arctic, J. Atmos. Sci., 59, 769–778, 2002. 3223, 3230
Gibson, J. K., Kallberg, P., Uppala S., Hernandez, A., Nomura, A., and Serrano, E.: ECMWF Re-Analysis Project Report Series, 1. ERA-15 Description, Version 2, ECMWF, Reading, UK, 1999. 3225
Hall, T. M. and Plumb, R. A.: Age as a diagnostic of stratospheric transport, J. Geophys. Res., 99, 1059–1070, 1994. 3225
Hurrell, J. W.: Decadal trends in the North Atlantic Oscillation: Regional temperatures and precipitation, Science, 269, 676–679, 1995. 3224, 3226, 3230
Hurrell, J. W., Kushnir, Y., Ottersen, G., and Visbeck, M. (Eds.): The North A tlantic Oscillation: Climate Significance and Environmental Impact, Geophysical Monograph Series, 134, 279, 2003. 3224, 3229
Leue, C., Wenig, M., Wagner, T., Klimm, O., Platt, U., and Jähne, B.: Quantitative analysis of NO_x emissions from Global Ozone Monitoring Experiment satellite image sequences, J. Geophys. Res., 106, 5493–5505, 2001. 3228
Li, C., Cornett, J., and K. Ungar: Long-term decrease of cadmium concentrations in the Canadian Arctic air, Geophys. Res. Lett., 30, 1256, doi: 10.1029/2002GL016723, 2003. 3224
Li, Q., Jacob, D.; Bey, I. et al.: Transatlantic transport of pollution and its effects on surface ozone in Europe and North America, J. Geophys. Res. 107, doi: 10.1029/2001JD001422, 2002. 3224
Meijer, S. N., Ockenden, W. A., Sweetman, A., Breivik, K., Grimalt, J. O., and Jones, K. C.: Global distribution and budget of PCBs and HCB in background surface soils: implications for sources and environmental processes, Environ. Sci. Technol., 37, 667–672, 2003. 3223
Mitchell, J. M.: Visual range in the polar regions with particulate reference to the Alaskan Arctic, J. Atmos. Terr. Phys. Special Suppl., 195–211, 1957. 3223
Monteith, D. T., Evans, C. D., and Reynolds, B.: Are temporal variations in the nitrate content of UK upland freshwaters linked to the North Atlantic Oscillation?, Hydrol. Process. 14, 1745–1749, 2000. 3231
Moritz, R. E., Bitz, C. M., and Steig, E. J., Dynamics of recent climate change in the Arctic, Science, 297, 1497-1502, 2002. 3230
Moulin, D., Lambert, C. E., Dulac F., and Dayan, U.: Control of atmospheric export of dust from North Africa by the North Atlantic Oscillation, Nature, 387, 691–694, 1997. 3224
Novelli, P. C., Masarie, K. A., and Lang, P. M.: Distributions and recent changes of carbon

monoxide in the lower troposphere, J. Geophys. Res., 103, 19 015–19 033, 1998. 3228
Olivier J. G. J., Bouwman, A. F., Van der Maas, C. W. M. et al.: Description of EDGAR Version 2.0. A set of global emission inventories of greenhouse gases and ozone depleting substances for all anthropogenic and most natural sources per country basis and on 1 × 1 grid, RIVM/TNO report, December 1996, RIVM Bilthoven, RIVM report no. 771060 002 (TNO MEP report no. R96/119), 1996. 3225
Pearl, H. W. and Whitall, D. R.: Anthropogenically-derived atmospheric nitrogen deposition, marine eutrophication and harmful algal bloom expansion: is there a link?, Ambio, 28, 307–311, 1999. 3230
Penkett, S. A. and Brice, K. A.: The spring maximum in photooxidants in the Northern Hemisphere troposphere, Nature, 319, 655–657, 1986. 3224
Polissar A., Hopke, P. K., and Harris J. M.: Source regions for atmospheric aerosol measured at Barrow, Alaska. Environ. Sci. Technol., 35, 4214–4226, 2001. 3224
Rossow, W. B. and Schiffer, R. A.: Advances in understanding clouds from ISCCP, Bull. Am. Met. Soc., 80, 2261–2287, 1999. 3228
Stohl, A., Eckhardt, S., Forster, C., James, P., and Spichtinger, N.: On the pathways and timescales of intercontinental air pollution transport, J. Geophys. Res., 107, 4684, doi: 10.1029/2001JD001396, 2002a. 3224, 3227
Stohl, A., Hittenberger, M., and Wotawa, G.: Validation of the Lagrangian particle dispersion model FLEXPART against large scale tracer experiment data, Atmos. Environ., 32, 4245–4264, 1998. 3225
Wang, X., and Key, J. R.: Recent trends in Arctic surface, cloud, and radiation properties from space, Science, 299, 1725–1728, 2003. 3230
Wania, F.: Assessing the potential of persistent organic chemicals for long-range transport and accumulation in polar regions, Environ. Sci. Technol., 37, 1344–1351, 2003. 3223

Table 1. Table shows coefficients obtained from a multiple linear regression with CO or BC as dependent, and time and NAO index as independent variables: a_1 intercept (unit ppbv for CO, ng m^{-3} for BC), a_2 trend (ppbv/year for CO, ng m^{-3}/year for BC), a_3 slope with NAO index (ppbv for CO, ng m^{-3} for BC). * significance of r^2 on the * 5% level, ** 1% level, *** 0.1% level

Station	Location	Period	Species	r^2	a_1	a_2	a_3
Mace Head	53.3° N 9.9 ° W	1991–2001	CO	0.27*	192	−4.2	−4.4
Mace Head	53.3° N 9.9 ° W	1989–2001	BC	0.49***	180	−3.1	−31.7
Spitsbergen	78.9° N 11.9° E	1994–2001	CO	0.41**	170	−0.9	3.3
Barrow	71.3° N 156.6° W	1994–2001	CO	0.44***	186	−2.4	4.0
Alert	82.5° N 62.5° W	1994–2001	CO	0.28**	187	−2.7	2.8

ACPD
3, 3222–3240, 2003

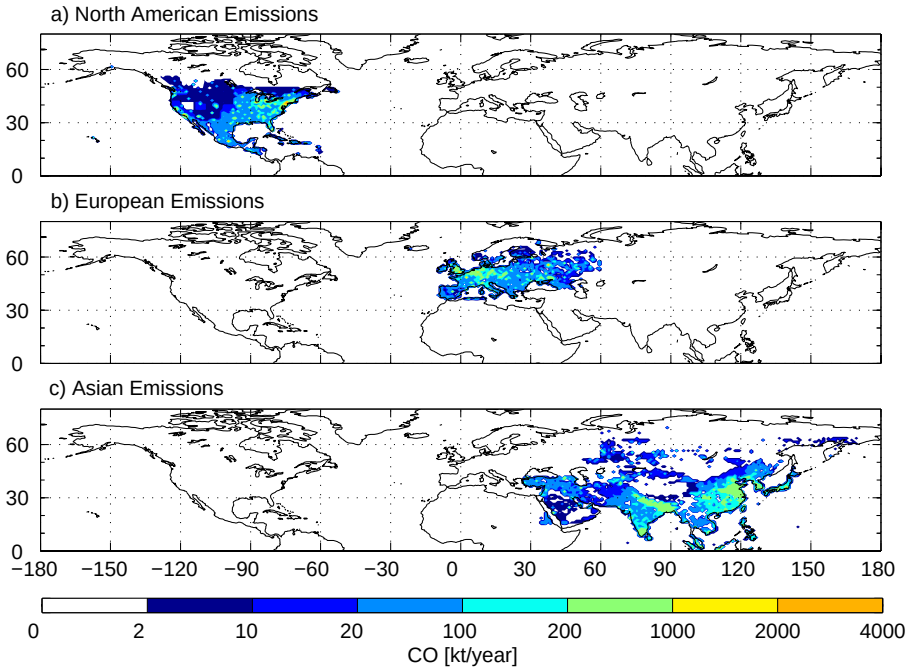

Fig. 1. Anthropogenic CO emissions in kilotons CO per year and 1° × 1° grid cell according to the EDGAR inventory for the base year 1990 for North America **(a)**, Europe **(b)** and Asia **(c)**.

ACPD
3, 3222–3240, 2003

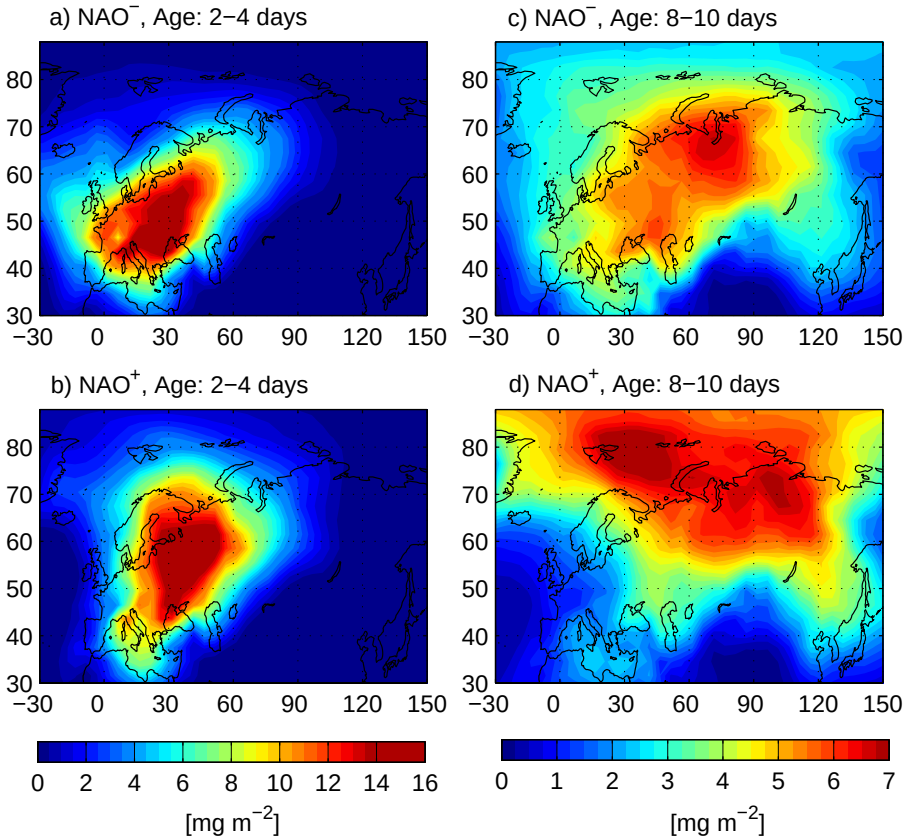

Fig. 2. European tracer columns [mg m^{-2}] 2–4 days (**a, b**), and 8–10 days (**c, d**) after tracer emission. The two composites represent the three December, January and February months with the lowest and highest NAO index, respectively, selected from a 15-year (1979–1993) period.

ACPD
3, 3222–3240, 2003

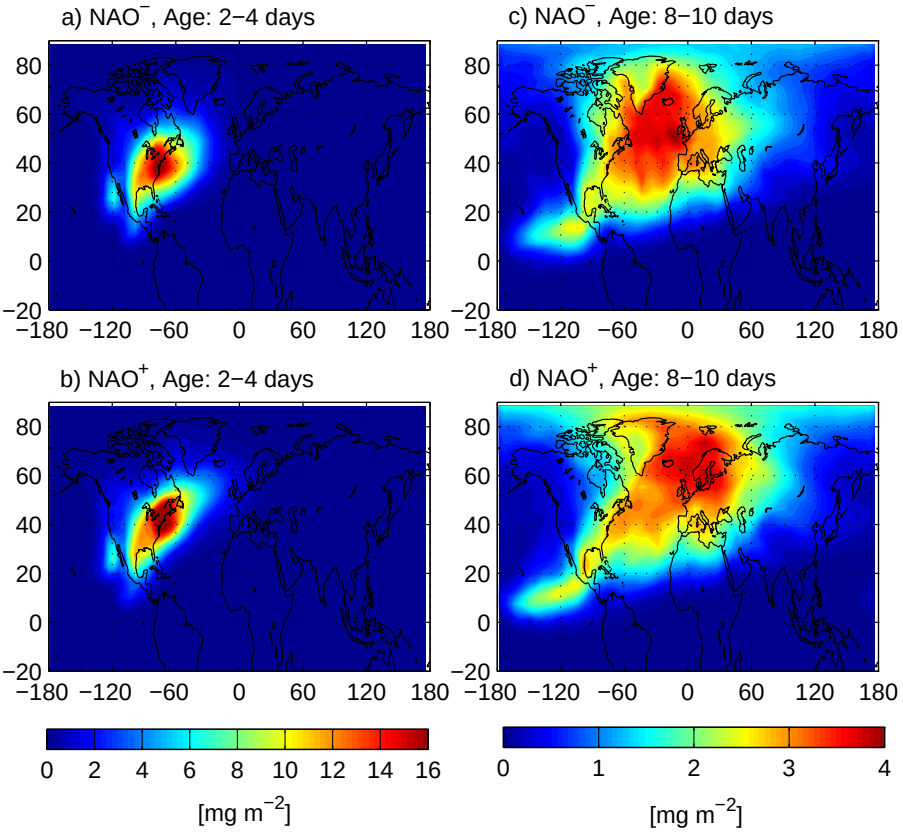

Fig. 3. Same as Fig. 2, but for the North American tracer.

ACPD
3, 3222–3240, 2003

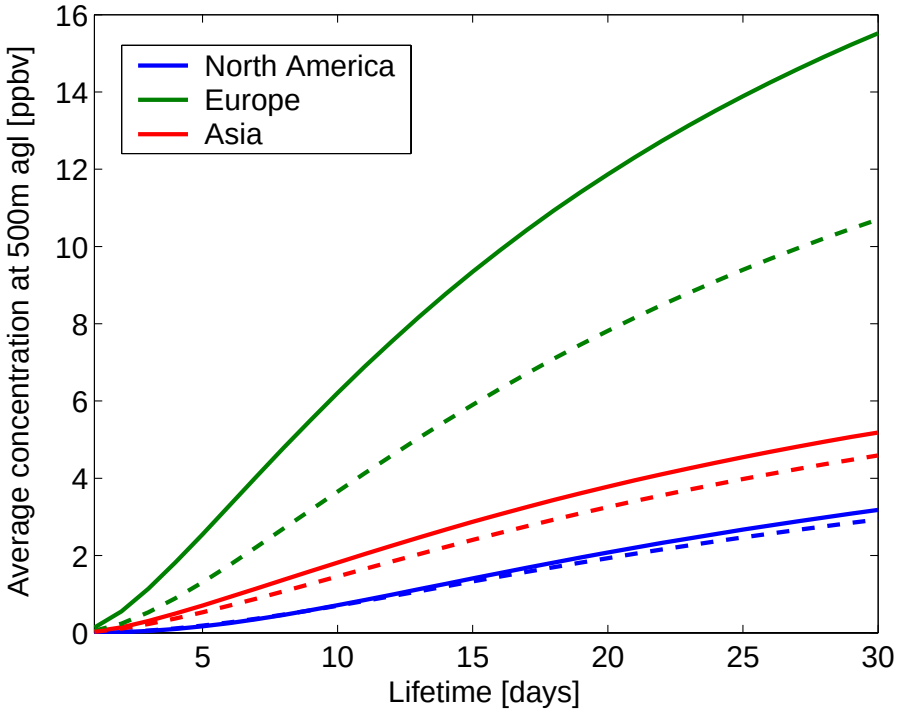

Fig. 4. Dependence of the winter-time mean tracer mixing ratios [ppbv] at the surface, averaged over the region north of 70° N, on tracer lifetime for NAO^+ (bold lines) and NAO^- (dashed lines) ensembles, respectively, for European (green lines), North American (blue lines) and Asian tracer (red lines).

ACPD
3, 3222–3240, 2003

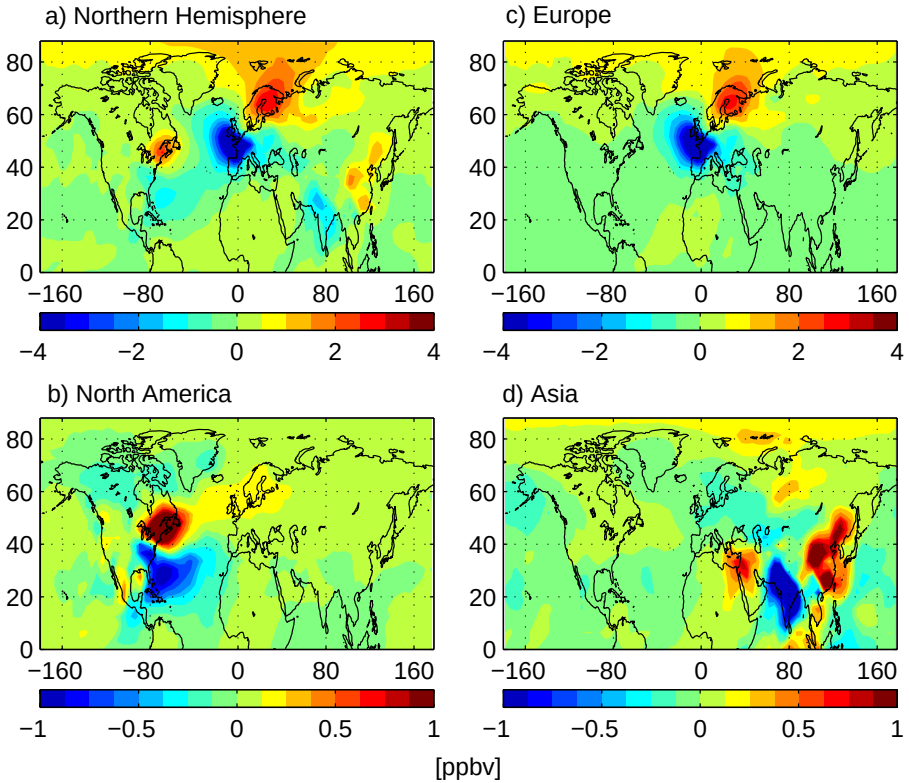

Fig. 5. Maps of the slopes (ppbv per index unit) between the 30-day-lifetime model tracer, and the NAO index in winter, for **(a)** all three NH source continents together, **(b)** North America alone, **(c)** Europe alone, and **(d)** Asia alone. The slopes were obtained by carrying out a linear regression analysis with the NAO index as the independent variable, and the tracer mixing ratio in the lowest model layer as the dependent variable.

ACPD
3, 3222–3240, 2003

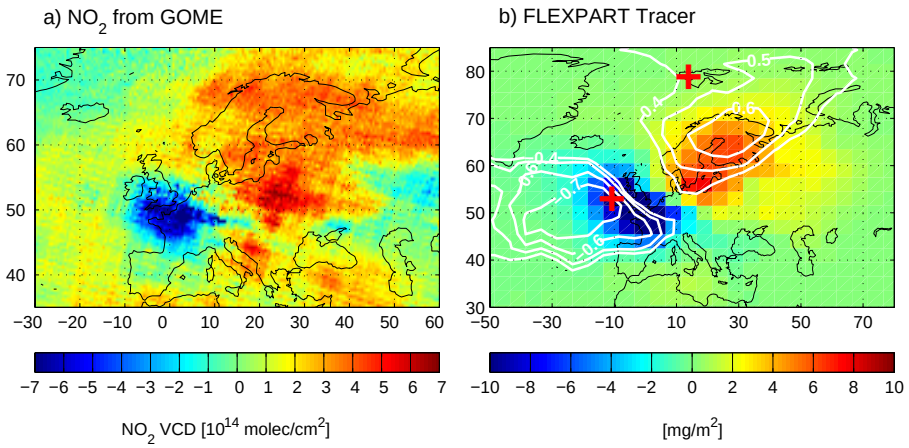

Fig. 6. Comparison of observed and simulated NAO signal in pollution transport from Europe. **(a)** Residuals of NO_2 columns retrieved from GOME satellite observations for NAO^+ minus NAO^- composites during seven (1996–2002) winters. **(b)** Map of the correlation coefficients between the NAO index and total vertical columns of the European 1-day-lifetime tracer (white contour lines) during 15 winters (1979–1993). The coloured isopleths represent the residuals of the tracer columns [mg m^{-2}] for NAO^+ minus NAO^- composites. Asterisks mark the locations of measurement sites at Mace Head and Spitsbergen.

ACPD
3, 3222–3240, 2003